LONGWALL MINE DESIGN WITH MULSIM/NL

By R. Karl Zipf, Jr.[1]

ABSTRACT

MULSIM/NL, developed by the U.S. Bureau of Mines (USBM), is a three-dimensional boundary-element-method computer program for stress analysis of coal mines. The PC-based program computes stresses throughout a mine. Engineers can then judge whether the stress levels are acceptable and, if not, adjust the mine layout accordingly. Users need material properties for coal, gob, and surrounding rock mass. In this paper, tables give suggested values for Young's modulus of the rock mass and suggested input parameters for strain-hardening gob, and figures give suggested input parameters for strain-softening coal. Different approaches are discussed for assigning material properties in MULSIM/NL models, namely: (1) uniform, (2) confinement, (3) width-to-height (w/h) ratio, and (4) combined. An example analysis of a longwall panel shows how to select and assign material properties to a model based on these suggestions. Discussions illustrate how to interpret the stress analysis results. A second example shows the analysis of a longwall panel that lies under old workings. The advantage of MULSIM/NL is that it can analyze complicated mine layouts, including multiple-seam interactions. The stress information provided by MULSIM/NL can help coal mining engineers avoid hazardous ground conditions, expensive repairs, and costly production delays due to inadequate mine planning.

INTRODUCTION TO MULSIM/NL

The USBM seeks to reduce ground control hazards and accidents to underground mineworkers through research on improved mine design. Numerical models provide coal mining engineers with a tool to test their intuition about the stress response of different underground mine layouts. The merits of alternate designs can then be judged from a ground control perspective.

This paper describes the capabilities of MULSIM/NL (*1-2*).[2,3] Next, detailed recommendations for material properties required by the computer program are provided. Finally, several examples illustrate application of MULSIM/NL for stress analysis of longwall panels. These examples illustrate the benefits of using the program in practical coal mine design.

MULSIM/NL uses the displacement-discontinuity approach (*3*) to calculate stresses and displacements around tabular deposits such as coal seams. References *1-3* provide details on the theory and operation of the program. MULSIM/NL can analyze from one to four parallel seams having any orientation with respect to the Earth's surface. These seams must lie far below the surface, since topographic or free surface effects are neglected. The user models each seam with a coarse-mesh grid of blocks (up to 50 by 50) that contains an embedded fine-mesh grid of elements (up to 150 by 150). Figure 1 shows a typical longwall coal mine layout and the modeling grid for a stress analysis using MULSIM/NL. The coarse-mesh blocks cover a large area of a mine layout, while the fine-mesh elements cover a central area where the user wants greater detail.

[1]Mining engineer, Denver Research Center, U.S. Bureau of Mines, Denver, CO.

[2]MULSIM/NL software and documentation are available from the author.

[3]Italic numbers in parentheses refer to items in the list of references at the end of this paper.

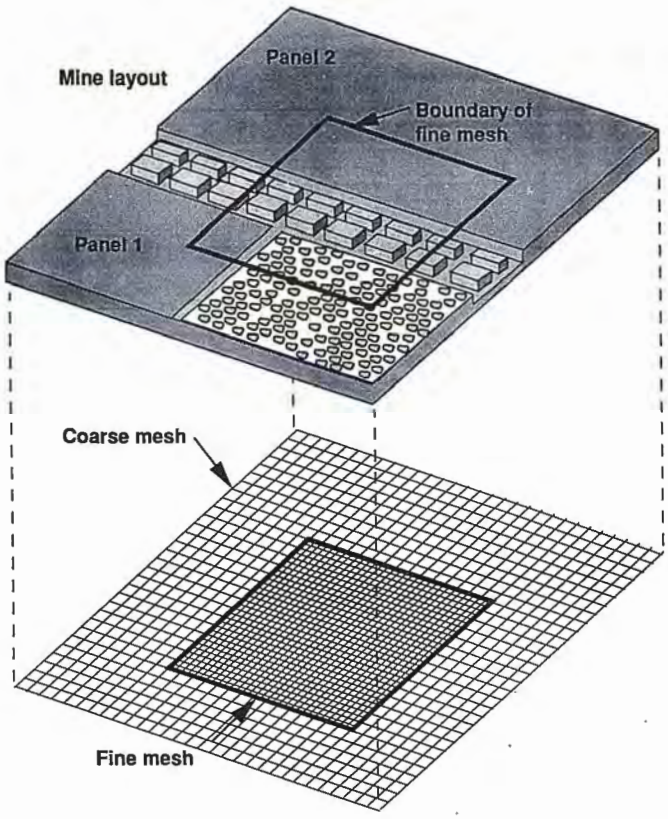

Figure 1.—Typical longwall coal mine layout and modeling grid for a stress analysis using MULSIM/NL.

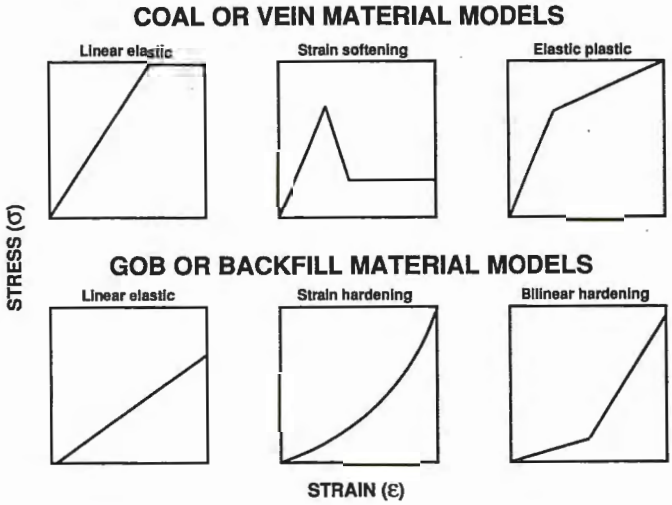

Figure 2.—Stress-strain models for MULSIM/NL.

NONLINEAR MATERIAL MODELS

MULSIM/NL assumes that a continuous, homogeneous, linear elastic rock mass surrounds the seam(s). Unlike prior versions of the program (*3-5*), which assume a linear elastic stress-strain relationship for the in-seam materials, MULSIM/NL now permits various nonlinear material models for the in-seam materials. Figure 2 shows the six models available for the in-seam material: linear elastic for intact seam material (coal), strain softening, elastic-plastic, bilinear hardening, strain hardening, and linear elastic for broken seam material (gob). The first three are intended for the unmined in-seam material, while the latter three are for the broken gob material left in the wake of full extraction mining (*1-2*).

MULTIPLE MINING STEPS AND ENERGY RELEASE CALCULATIONS

MULSIM/NL has a multiple mining step capability to simulate the various stages of mining. With this feature, the user can compute and examine stress and displacement changes between mining steps. Such changes are more comparable to field measurements that usually record stress and displacement changes, as opposed to total, or absolute, stresses and displacements. Based on stress and displacement changes between mining steps, MULSIM/NL computes an energy release rate (ERR) using the derivations of Salamon (*6*). ERR may serve as an indicator of coal mine bump risk (*7*). In addition, MULSIM/NL calculates other strain energy quantities that may serve as indicators of coal mine bump potential (*1, 8*).

INPUT PARAMETERS FOR MULSIM/NL

To conduct a stress analysis with MULSIM/NL, the user must first define the mine geometry of interest to the computer program. The subsequent examples will help to illustrate how this part of an analysis is done. In addition, the user must supply material properties data to the program for the coal, the gob, and surrounding rock mass. Choosing acceptable values for these crucial input parameters will help to ensure that the user obtains a reasonable approximation to the stresses at a particular site.

For the rock mass surrounding the coal seam, the major input parameter required is the Young's modulus. MULSIM/NL assumes that the surrounding rock mass is a linear elastic, homogeneous continuum. Table 1 provides a suggested range of Young's modulus values for different coal measure rocks. The user may have

laboratory measurements of the Young's modulus available. Laboratory-scale values usually exceed field-scale values by a factor of one to four. Typically, the user must decrease a laboratory value by about 50% to obtain the equivalent field-scale value for rock mass modulus.

Table 1.—Suggested values for Young's modulus of rock mass

Major component of rock mass	Range for Young's modulus	
	MPa	psi
Shale	2,000- 6,000	300,000- 900,000
Siltstone	4,000- 9,000	600,000-1,300,000
Sandstone	6,000-12,000	900,000-1,800,000

For the gob left in the wake of full extraction mining, the user must select one of the three different material models available for the gob. The linear elastic and the strain-hardening models are the usual choices. The bilinear hardening model is for special applications. It is highly recommended that the user begin new MULSIM/NL analyses using the linear elastic model. Suggested values for the Young's modulus of the gob might range from 35 to 350 MPa (5,000 to 50,000 psi). After some initial analyses using a linear elastic gob model are complete, the user may want to improve the stress calculations by selecting the more realistic strain-hardening material model for the gob. This model requires three main parameters: an initial tangent modulus, a final tangent modulus, and the vertical stress at that final modulus. Recent laboratory work by Pappas and Mark (*9*) provides a basis for selecting input parameters to the strain-hardening gob model. Table 2 summarizes a suggested range of values for these parameters.

Table 2.—Suggested values for strain-hardening gob model

Parameter	Range	
	MPa	psi
Initial tangent modulus	2- 10	300- 1,500
Final tangent modulus	150-250	20,000-35,000
Final stress	15	2,200

For the coal, the user again has a choice of three different material models: linear elastic, strain-softening, and elastic-plastic. The linear elastic and the strain-softening models are the usual choices. The elastic-plastic model is actually just a special case of the more general strain-softening model. Again, it is highly recommended that the user begin new MULSIM/NL analyses with the linear elastic model. Suggested values for the Young's modulus values of the coal might range from 1,500 to 4,000 MPa (200,000 to 600,000 psi). After some initial analyses using a linear elastic coal model are complete, the user may want to improve the stress calculations by selecting the more realistic strain-softening material model for the coal. This model requires four main parameters: a peak stress and strain, and a residual stress and strain. These parameters define the two points of a strain-softening, stress-strain curve for the coal material as shown in figure 2. Published strength data on full-scale coal pillars provide the basis for selecting these important parameters.

Numerous researchers have created empirical formulas for the strength of coal pillars as a function of the w/h ratio. Bieniawski and van Heerden (*10*) established the linear relationship shown in figure 3 for the peak strength of coal pillars. Recent research by Maleki (*11*) established a

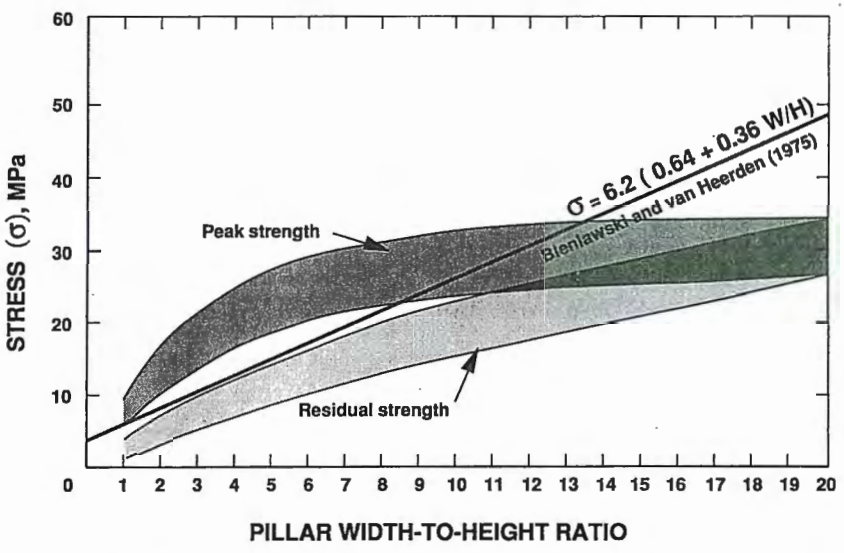

Figure 3.—Strength of coal pillars as a function of width-to-height (W/H) ratio. Peak and residual strengths after Maleki (*11*).

range for the peak and residual pillar strengths as a function of w/h ratio, also shown in figure 3. According to Maleki, the high-strength curve is typical for mines with a large degree of pillar confinement, while the low-strength curve is typical for structurally controlled coal seams with persistent cleats and in-seam contact planes. As shown in figure 4, various researchers (*14-18*) have also contributed data on the postfailure modulus of coal pillars as a function of w/h ratio. By assuming an initial elastic modulus of 2,750 MPa (400,000 psi) and combining the peak and residual strength data of Maleki (*11*) with the postfailure modulus data shown in figure 4, we obtain a set of low-range (figure 5) and a set of high-range (figure 6) strain-softening stress-strain curves for coal that depend on the w/h ratio. Figures 5 and 6 provide a range of suggested values for the peak stress and strain and the residual stress and strain parameters required by the strain-softening material model in MULSIM/NL. Again, the curves shown in figures 5 and 6 are merely suggested places to start. They are based on limited data that exhibit tremendous variance. Whenever possible, the user should obtain site-specific data based on in-mine observations.

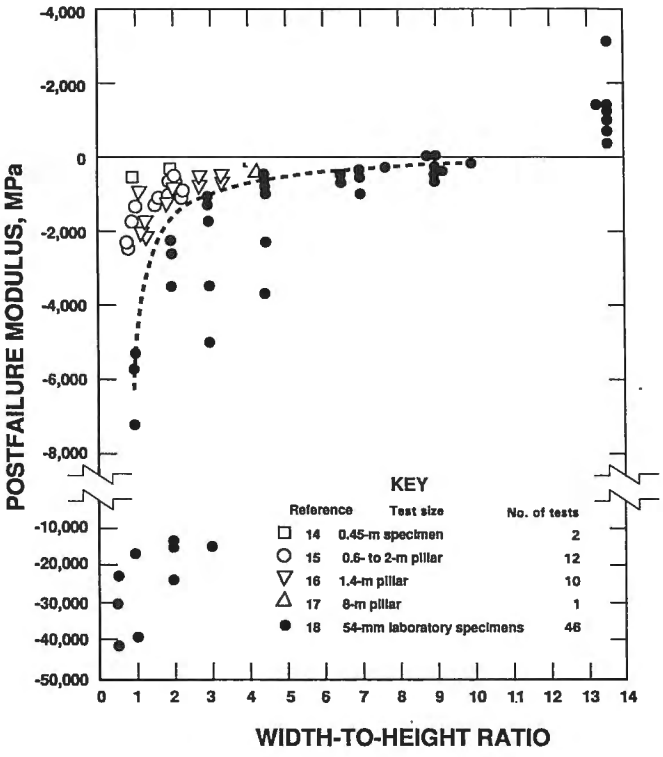

Figure 4.—Postfailure modulus data as a function of w/h ratio.

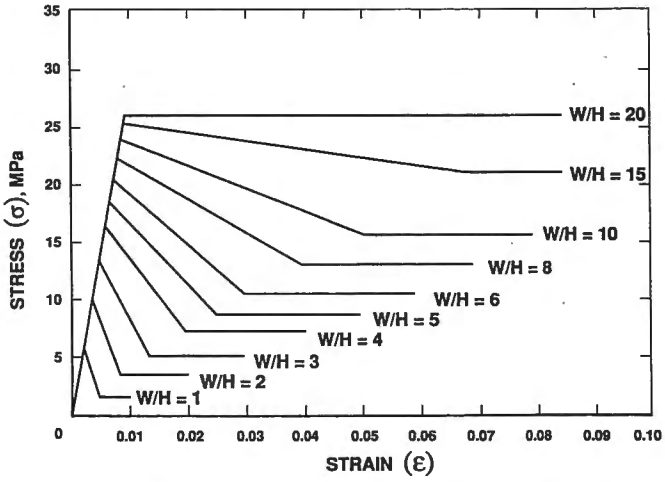

Figure 5.—Suggested strain-softening stress-strain models for MULSIM/NL: low range.

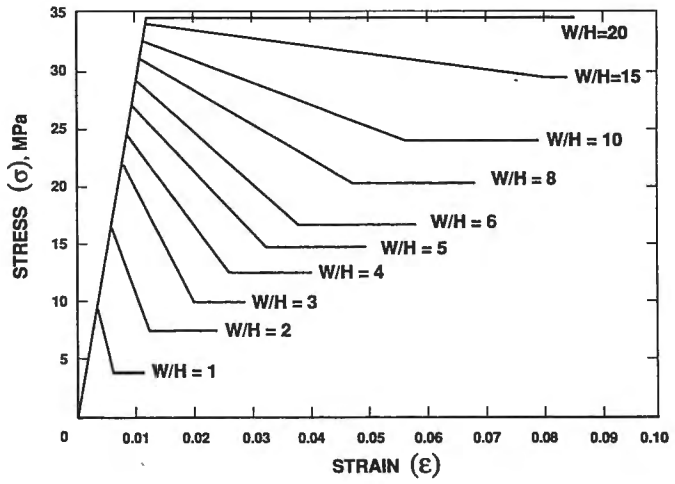

Figure 6.—Suggested strain-softening stress-strain models for MULSIM/NL: high range.

MODELING STRATEGIES WITH MULSIM/NL

In using MULSIM/NL for conducting stress analyses of coal mines, the user must assign material properties to each element in a model. In assigning these properties to the coal elements, four different approaches can be followed: (1) uniform, (2) confinement, (3) w/h ratio, and (4) combined. Figure 7 shows the layout of the headgate area between two longwall panels and indicates how the assignment of material properties defines the mine geometry in a MULSIM/NL model. In the uniform approach shown in figure 7, the same stress-strain curve is applied to a material throughout the mine geometry. In this example, material A is linear elastic coal, and material B is linear elastic gob. However, A could just as well be a strain-softening material, and B could be a strain-hardening material. In any case, properties for coal and gob are uniform throughout the model. The uniform materials approach is usually used for the initial MULSIM/NL stress analyses of a model. Cox and others (*12*) provide an example of this approach using a uniform strain-softening model.

In the confinement approach shown in figure 8, the user assigns different material properties to the elements based on their distance to an opening. Coal elements that are 0 to 3 m (0 to 10 ft) from an opening follow stress-strain curve A, those that are 3 to 6 m (10 to 20 ft) follow stress-strain curve B, and those that are 6 m (20 ft) or more follow stress-strain curve C. This approach accounts directly for the effects of confinement on the strength and postfailure properties of the coal. However, the user should have available stress measurements at various depths into a pillar to help formulate strain-softening stress-strain curves for input. Zipf and Heasley (*7*), Heasley (*8*), Heasley and Zelanko (*13*), and Cox and others (*12*) provide examples of the confinement approach in their analyses using MULSIM/NL.

In the w/h ratio approach shown in figure 9, the user assigns different material properties to entire pillars based on the w/h ratio of the pillar. Thus, the yield pillar with a w/h ratio of 3 follows stress-strain curve A, which is highly strain-softening; the abutment pillar with a w/h

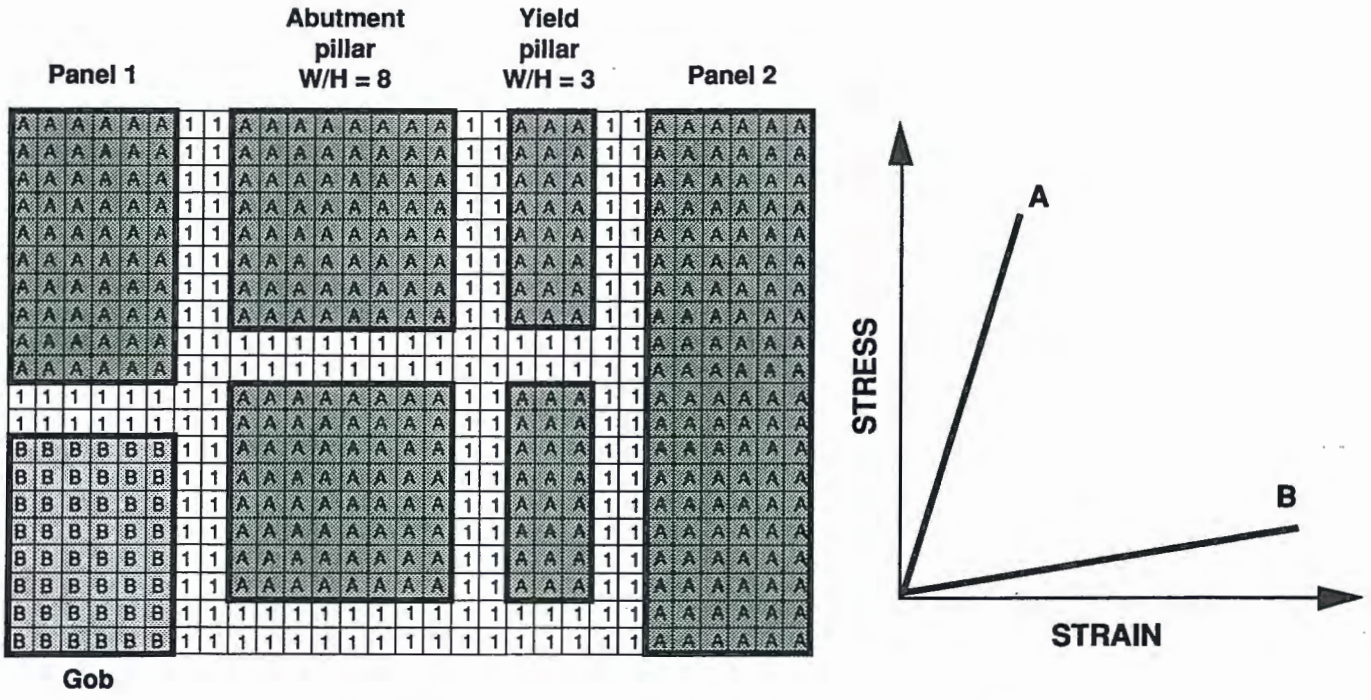

Figure 7.—Uniform approach for material modeling with MULSIM/NL.

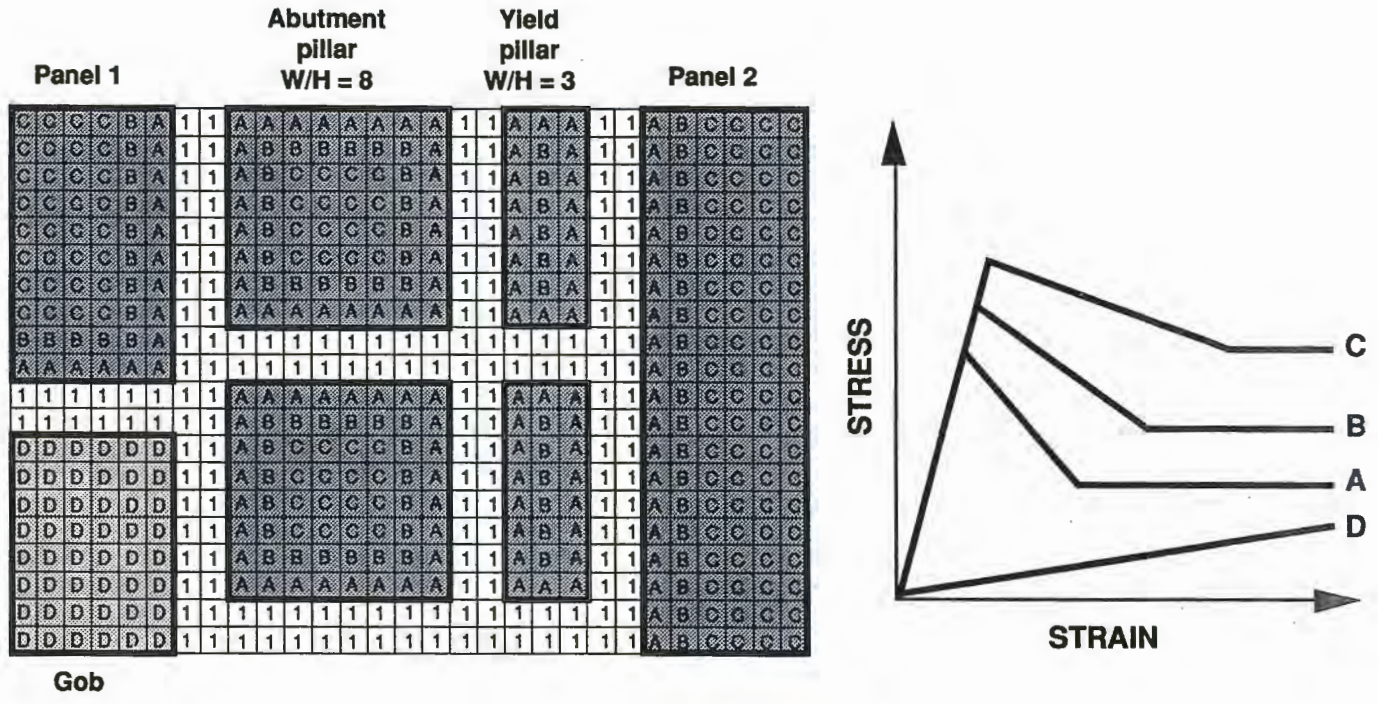

Figure 8.—Confinement approach for material modeling with MULSIM/NL.

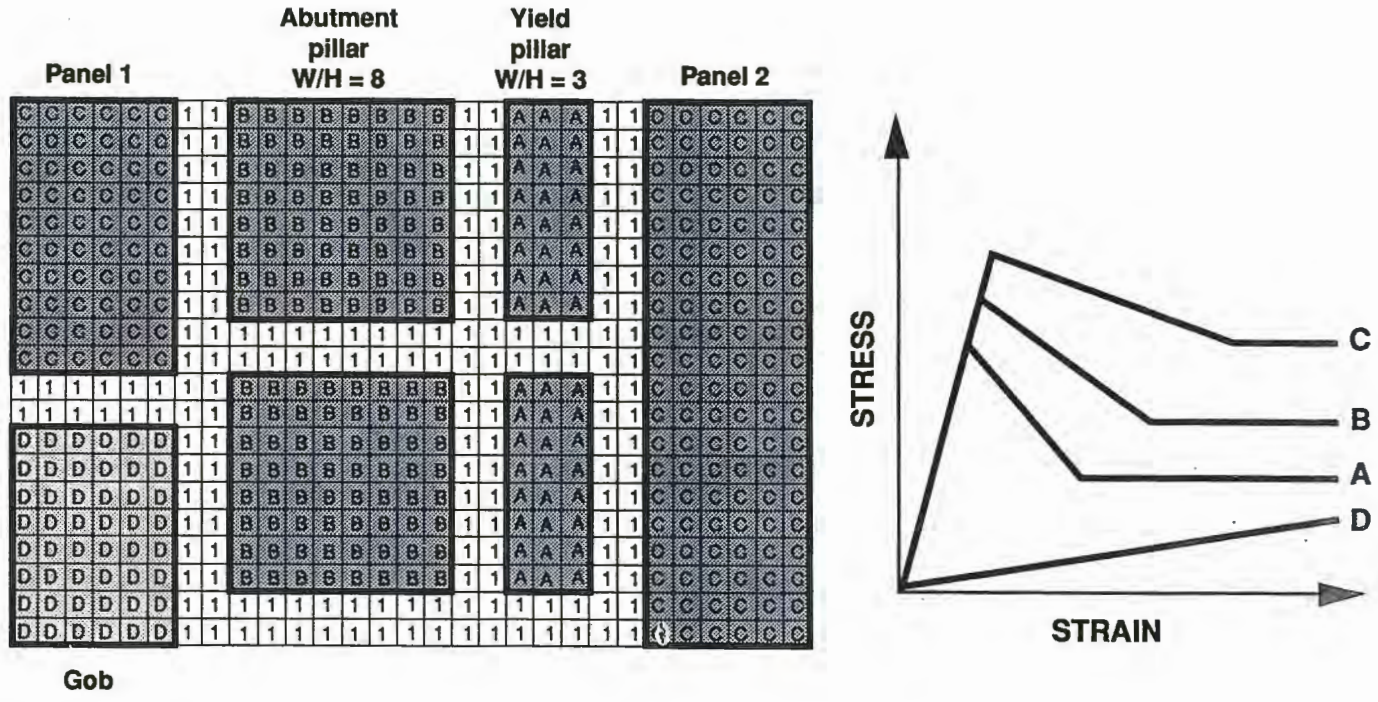

Figure 9.—Width-to-height ratio approach for material modeling with MULSIM/NL.

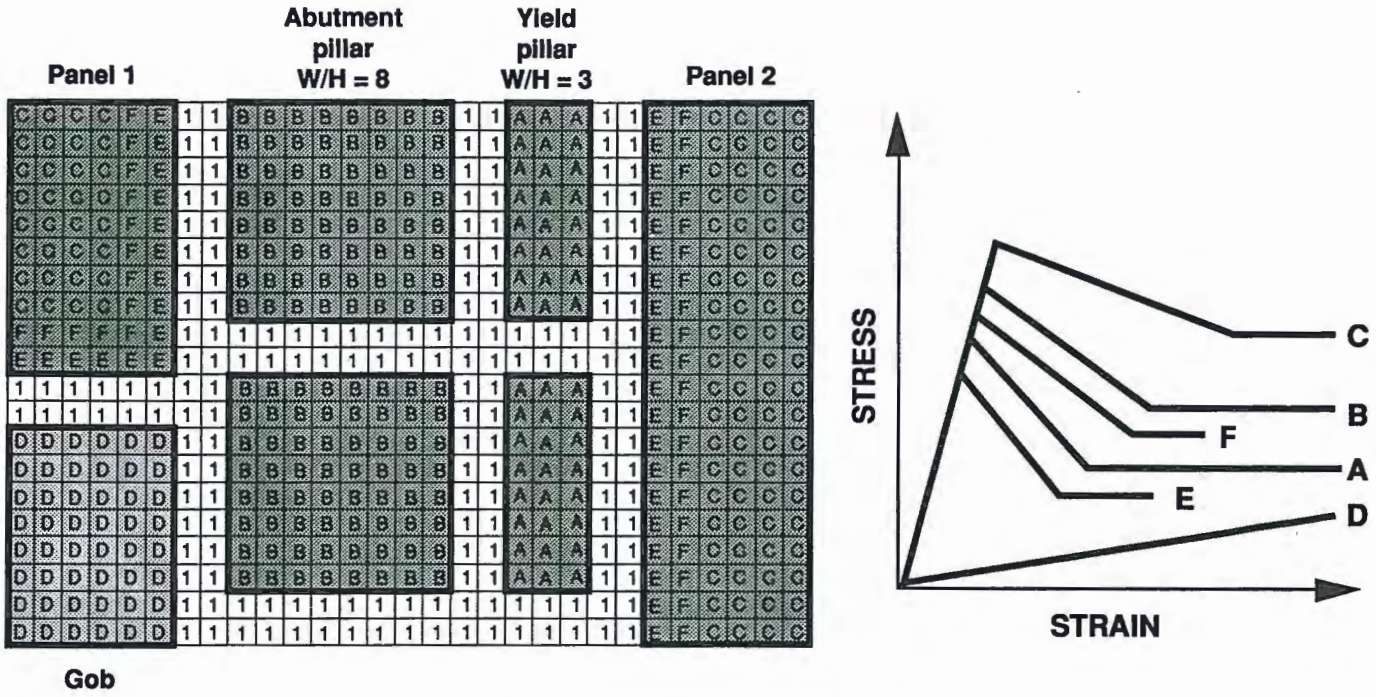

Figure 10.—Combined approach for material modeling with MULSIM/NL.

ratio of 8 follows curve B, which is moderately strain softening; and the solid abutment areas with a w/h ratio greater than 20 follow curve C, which is nearly elastic-plastic. The w/h ratio accounts for the effects of confinement indirectly. The advantage to this approach is the large amount of pillar strength data as a function of w/h ratio that are available. Figures 5 and 6, discussed earlier, provide a range of suggested strain-softening stress-strain curves that depend on w/h ratio. The example analyses provided in this paper illustrate the w/h ratio approach when using MULSIM/NL for stress analysis.

The combined approach shown in figure 10 uses aspects of the confinement and the w/h ratio approaches to assign material properties in a model. One problem with the w/h ratio approach is that it may not work well for pillars with a w/h ratio greater than 20, such as the solid abutment areas around a coal panel. The combined approach overcomes this problem by assigning material properties to solid abutment areas using the confinement approach. Pillars with a w/h ratio less than 20 are still assigned material properties on the basis of their w/h ratio. Therefore, the combined approach tends to bring together the best features of both the confinement and the w/h ratio approaches.

EXAMPLE ANALYSES OF LONGWALL MINES WITH MULSIM/NL

Using MULSIM/NL, an engineer can conduct realistic stress analyses of complex longwall gate road systems, provided that correct material properties are used. Such analyses can help to ensure adequate pillar stability throughout the life of the longwall gate road system. Figures 11, 12, and 13 show computed vertical stresses across complete longwall panels. In these example analyses, mining progresses from left to right. The headgate entries are near the bottom of the model, while the tailgate entries are near the top. All gate road systems use three entries with one 9-m- (30-ft-) wide yield pillar and an abutment pillar that is 18 m (60 ft) square in figure 11, 24 m (80 ft) square in figure 12, and 30 m (100 ft) square in figure 13. Mining occurs at a depth of 300 m (1,000 ft), where the in situ vertical stress is about 7.5 MPa (1,100 psi). Seam thickness is approximately 3 m (10 ft). These MULSIM/NL models show behavior of the gate road pillars at all stages of their life. In the area labeled A in the figures, pillars bear development loads only. In areas B and C, pillars are subject to side abutment loads due to

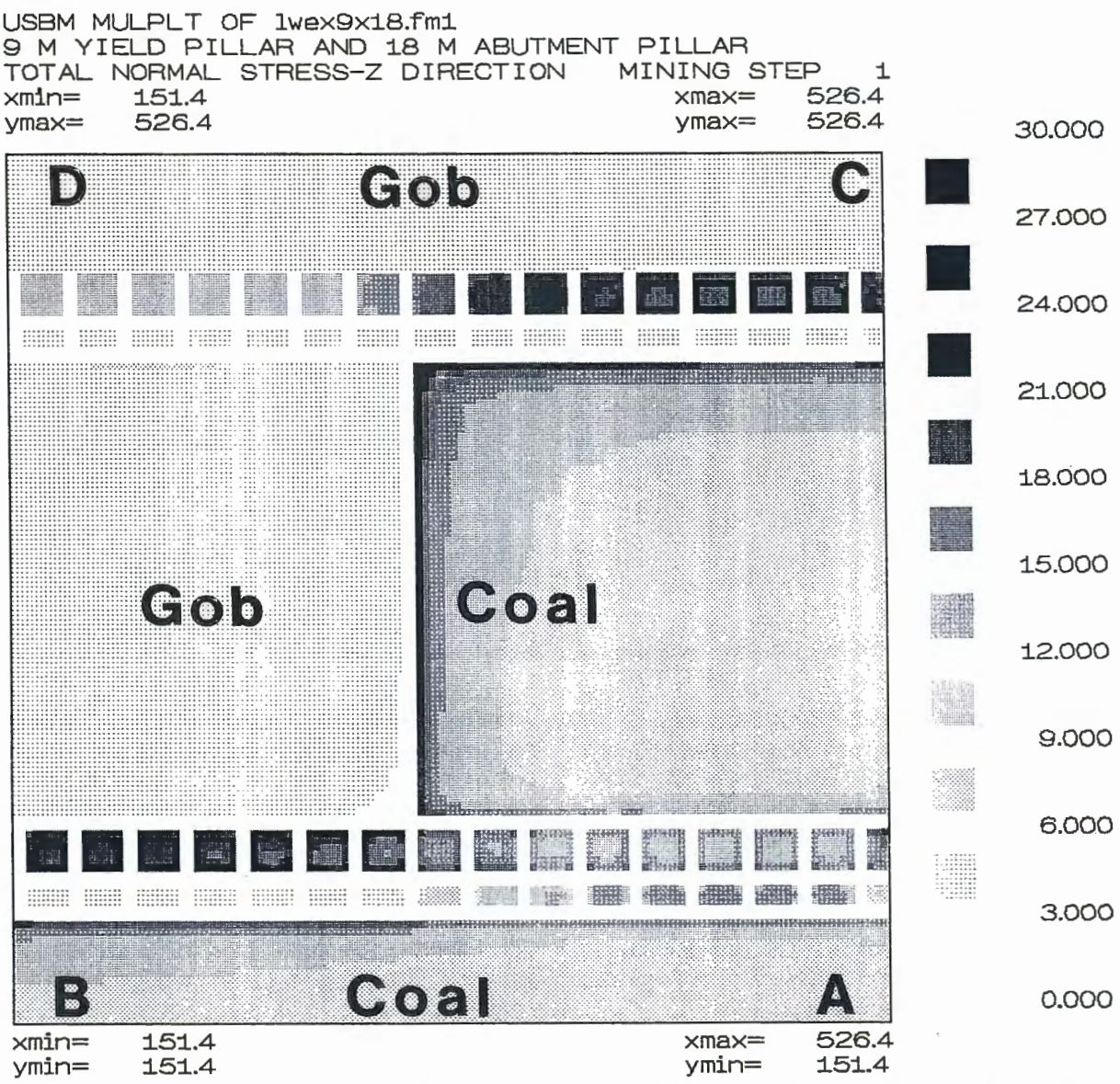

Figure 11.—Computed stresses in MPa across longwall panel with 9-m (30-ft) yield pillar and 18-m (60-ft) abutment pillar. (1 MPa = 145 psi.)

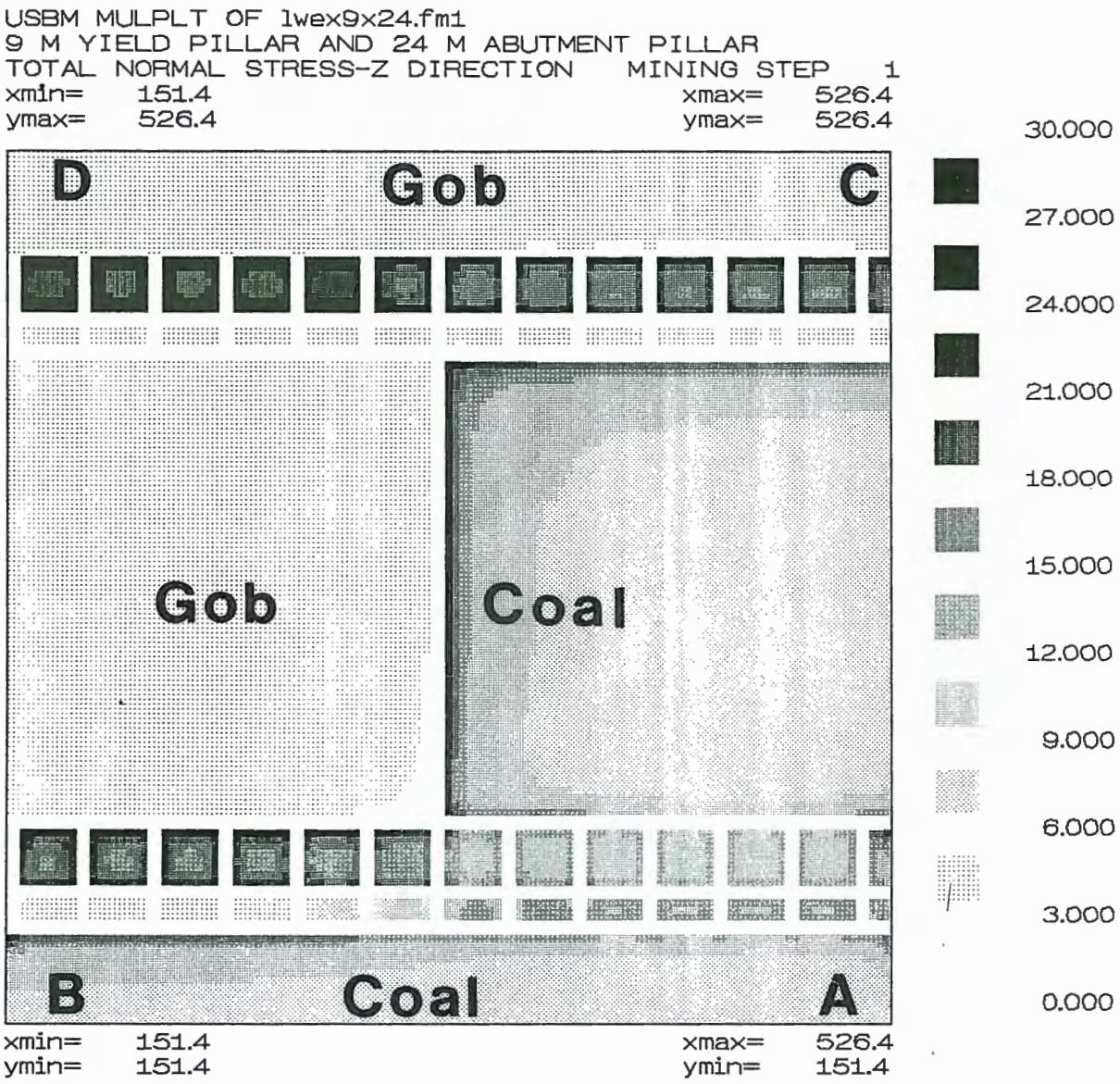

Figure 12.—Computed stresses in MPa across longwall panel with 9-m (30-ft) yield pillar and 24-m (80-ft) abutment pillar. (1 MPa = 145 psi.)

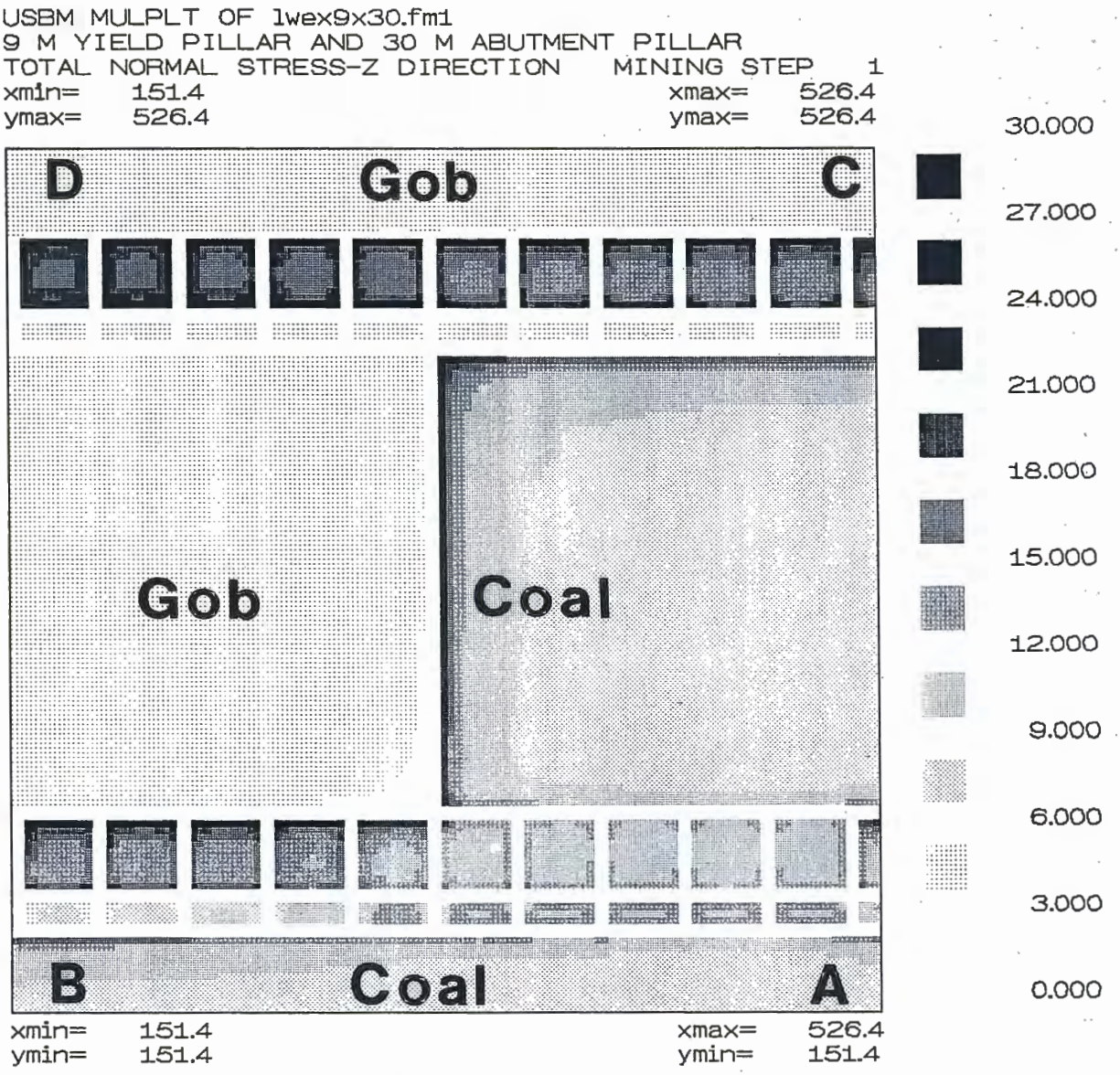

Figure 13.—Computed stresses in MPa across longwall panel with 9-m (30-ft) yield pillar and 30-m (100-ft) abutment pillar. (1 MPa = 145 psi.)

first panel mining. Finally, in area D, pillars experience a second side abutment load due to second panel mining.

MULSIM/NL requires estimates for certain mechanical properties of the coal and the surrounding rock mass. In these analyses, initial elastic modulus of the coal is 2,750 MPa (400,000 psi). Modulus of the rock mass is 10,000 MPa (1,450,000 psi). All analyses use the strain-softening material model for the in-seam coal, which requires an estimate of the peak and residual strength for the coal. Figures 5 and 6 discussed earlier provide a rational means to estimate these strengths as a function of the w/h ratio of the pillar. Table 3 shows the peak and residual strength values for the different pillar sizes used in these analyses.

Figure 11 shows vertical stresses computed by MULSIM/NL for a gate road system using an 18-m (60-ft) abutment pillar with a 9-m (30-ft) yield pillar. On the headgate side, MULSIM/NL shows that the yield pillar begins to fail about 50 m (160 ft) ahead of the face. In other words, the yield pillar has exceeded its peak strength, and the stresses now equal its residual strength. Stresses on the 18-m (60-ft) abutment pillar continue to increase as the longwall face approaches. After the face passes, the abutment pillar begins to fail adjacent to the gob, where stresses have decreased to the residual strength. After first panel mining, in the areas labeled B and C in the figure, MULSIM/NL indicates very high stresses in the core of the abutment pillar. On the tailgate side, the stress calculations show that the 18-m (60-ft) abutment pillar reaches it peak strength about 75 m (240 ft) ahead of the face. In addition, high stress levels exist on the longwall face at the tailgate corner. These stress calculations indicate that the yield pillar fails completely and the abutment pillar fails partially before completion of second panel mining. Therefore, this gate road geometry may be unacceptable.

Figure 12 shows vertical stresses computed by MULSIM/NL for the gate road system using a 24-m (80-ft) abutment pillar with a 9-m (30-ft) yield pillar. With this gate road geometry, the yield pillar fails completely on the headgate side about 30 m (100 ft) after passage of the longwall face. Stresses on the 24-m (80-ft) abutment pillar increase as the longwall face approaches; however, it does not begin to fail as the 18-m (60-ft) abutment pillar did. This pillar remains intact after first panel mining as indicated near areas B and C in the figure. In addition, stress levels on the longwall face at the tailgate corner have decreased because of the larger abutment pillar. As the face approaches on the tailgate side, stresses on the abutment pillar increase. However, unlike the prior case with the 18-m (60-ft) abutment pillar, the 24-m (80-ft) abutment pillar survives after passage of the longwall face. Therefore, this gate road geometry is probably acceptable.

Lastly, figure 13 shows vertical stresses computed by MULSIM/NL for the gate road system using a 30-m (100-ft) abutment pillar with a 9-m (30-ft) yield pillar. With this gate road geometry, the yield pillar fails completely on the headgate side about 130 m (425 ft) after passage of the longwall face. Stresses on the 30-m (100-ft) abutment pillar increase as the longwall face approaches, and as before, it does not fail. This pillar remains intact after first panel mining as indicated near the areas labeled B and C in the figure. Stress levels on the longwall face at the tailgate corner are about the same as with the 24-m (80-ft) abutment pillar. As the face approaches on the tailgate side, stresses on the abutment pillar continue, but it does not fail after passage of the longwall face. Therefore, this gate road geometry is also acceptable, although it is somewhat more conservative than the prior geometry.

One must be cautioned that the accuracy of the stress predictions calculated by MULSIM/NL depends on the material properties selected by the user. The methods for choosing these properties suggested herein are a good place to start; however, the user should always attempt to verify these predictions with field observations and make adjustments accordingly.

Table 3.—Peak and residual strength values for pillars

Pillar type and size	Width-to-height ratio	Peak strength		Residual strength		Figure example
		MPa	psi	MPa	psi	
Yield: 9 m ...	3	15	2,200	5	700	All
Abutment:						
18 m	6	22.5	3,300	10	1,500	11
24 m	8	26	3,800	15	2,200	12
30 m	10	29	4,200	20	2,900	13
Solid coal	NAp	31	4,500	31	4,500	All

NAp Not applicable.

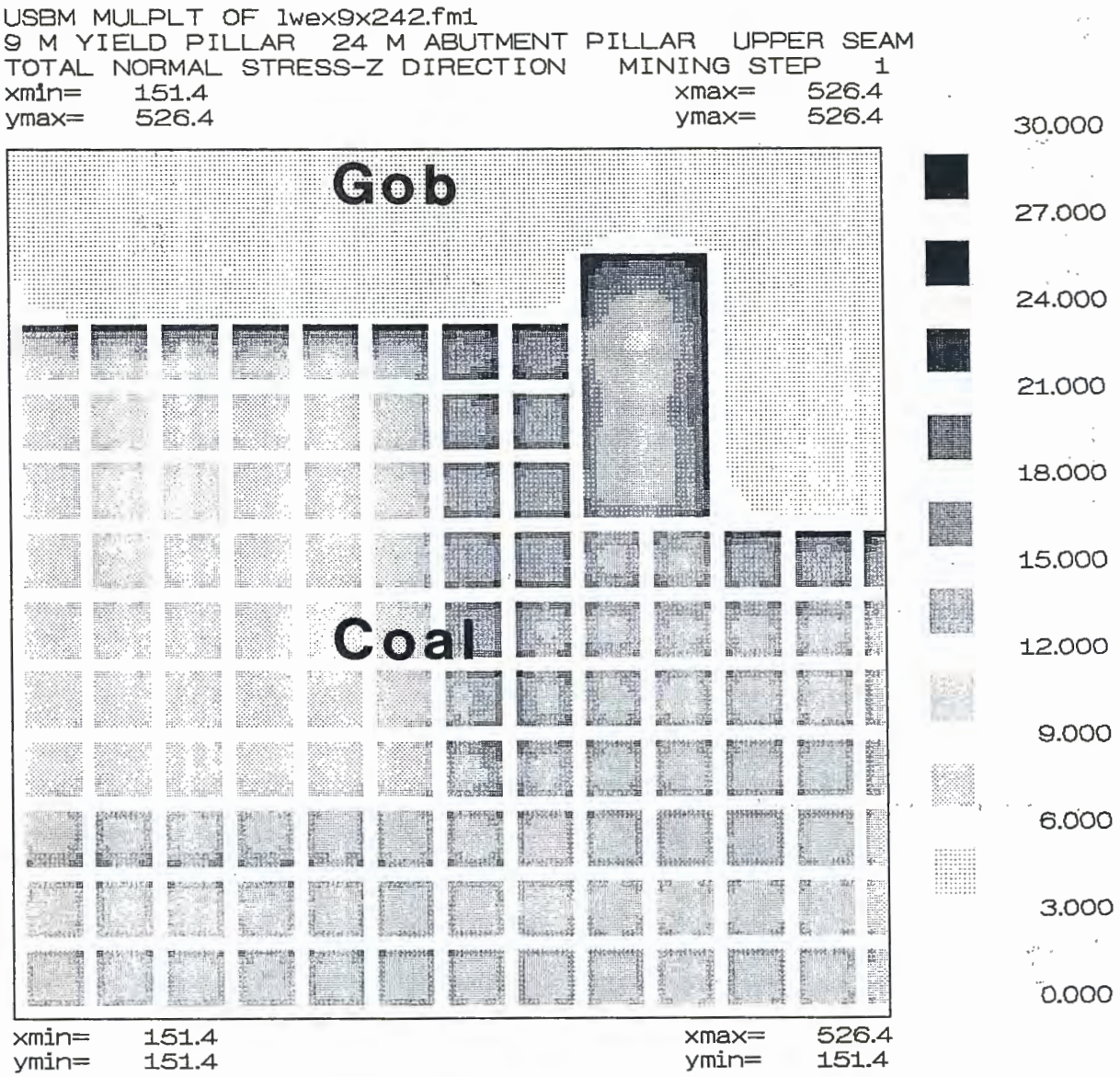

Figure 14.—Computed stresses in MPa across room-and-pillar workings of upper seam. (1 MPa = 145 psi.)

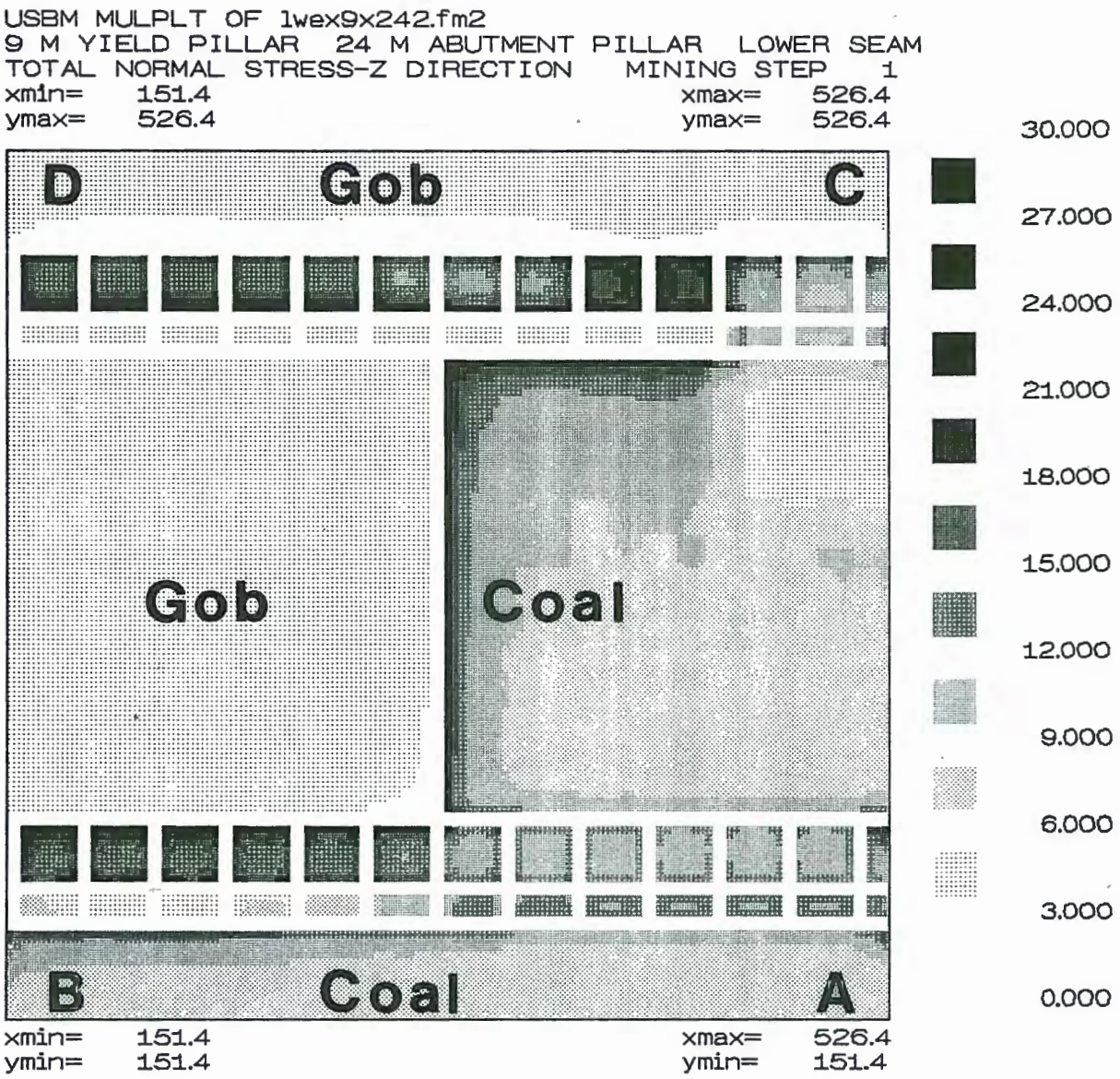

Figure 15.—Computed stresses in MPa across longwall panel of lower seam with 9-m (30-ft) yield pillar and 24-m (80-ft) abutment pillar. (1 MPa = 145 psi.)

The advantage of MULSIM/NL is its ability to analyze stresses for complicated mine geometries and multiple-seam interactions. Figures 14 and 15 illustrate a stress analysis for multiple-seam mining scenarios. Figure 14 shows computed stresses for the upper seam that has been partially extracted with room-and-pillar mining. A large barrier pillar remains adjacent to the gob. Figure 15 shows the stresses on the lower seam, which is 20-m (66-ft) below the upper seam. This longwall mine uses 9-m (30-ft) yield pillars with 24-m (80-ft) abutment pillars and is identical to the operation shown in figure 12. In figure 14, undermining in the lower seam has caused stresses in the upper pillars to decrease. Otherwise, the stress distribution in the upper seam is typical, with higher stresses adjacent to the gob and in the large barrier pillar.

The presence of mining in the upper seam causes numerous changes to the stress distribution in the lower seam. (Figure 12 shows the stresses within this seam without any mining in the upper seam.) In comparing figures 12 and 15, stresses in the headgate pillars and on the headgate side of the longwall panel near areas A and B remain unchanged by the partial extraction in the upper seam. However, the abutment pillars in the tailgate, which lie partially under the gob in the upper seam, show a decrease in stresses. In the area labeled C, figure 12 indicates average abutment pillar stresses of 15 to 18 MPa (2,200 to 2,600 psi), whereas figure 15 shows stresses of 12 to 15 MPa (1,700 to 2,200 psi). The decrease is even more profound in area D. Figure 12, without upper-seam mining, indicates average stresses of about 21 to 24 MPa (3,000 to 3,500 psi), whereas figure 15, with upper-seam mining, shows lower average stresses of about 12 to 15 MPa (1,700 to 2,200 psi).

The presence of the barrier pillar causes many changes to the stress distribution in the lower seam that may affect the mining operations. As seen in figure 15, stresses in the tailgate abutment pillars directly under the barrier pillar have higher stress levels. The stresses in these pillars are identical to those found in figure 12 near area D where the abutment pillars are subject to full-side abutment stresses from both longwall panels. In addition, stresses on the tailgate side of the longwall face are higher than those in the single-seam case. The high stresses under the barrier pillar may cause ground control problems in that section of the tailgate. Extra mine roof support, such as cable bolts or cribs, may be necessary.

SUMMARY

MULSIM/NL, available from the USBM, performs stress analysis of coal mines. As shown in the example analyses, it can calculate realistic stress distributions over a wide variety of complicated longwall mining geometries. These stress distributions can indicate those parts of the mine that have failed and those that remain intact. However, the coal mining engineer must verify the MULSIM/NL predictions against field observations at the mine prior to using the model in new mining areas. The stress analyses provided by MULSIM/NL can help mining companies avoid hazardous ground conditions and costly production delays brought about through inadequate ground control planning.

REFERENCES

1. Zipf, R. K., Jr. MULSIM/NL Theoretical and Programmer's Manual. USBM IC 9321, 1992, 52 pp.

2. ____. MULSIM/NL Application and Practitioner's Manual. USBM IC 9322, 1992, 48 pp.

3. Sinha, K. P. Displacement Discontinuity Technique for Analyzing Stresses and Displacements Due to Mining Seam Deposits. Ph.D. Thesis, Univ. MI, Ann Arbor, MI, 1979, 311 pp.

4. Beckett, L. A., and R. S. Madrid. MULSIM/BM—A Structural Analysis Computer Program for Mine Design. USBM IC 9168, 1988, 302 pp.

5. Donato, D. A. MULSIM/PC—A Personal-Computer-Based Structural Analysis Program for Mine Design in Deep Tabular Deposits. USBM IC 9325, 1992, 56 pp.

6. Salamon, M. D. G. Energy Considerations in Rock Mechanics: Fundamental Results. J. S. Afr. Inst. Min. and Metall., v. 84, No. 8, 1984, pp. 233-246.

7. Zipf, R. K., and K. A. Heasley. Decreasing Coal Bump Risk Through Optimal Cut Sequencing with a Non-Linear Boundary Element Program. Paper in Proceedings of the 31st U.S. Symp. on Rock Mechanics (CO Sch. Mines). A. A. Balkema, Rotterdam, 1990, pp. 947-954.

8. Heasley, K. A. An Examination of Energy Calculations Applied to Coal Bump Prediction. Paper in Proceedings of the 32nd U.S. Symposium on Rock Mechanics (Univ. OK). A. A. Balkema, Rotterdam, 1991, pp. 481-490.

9. Pappas, D. M., and C. Mark. Behavior of Simulated Longwall Gob Material. USBM RI 9458, 1993, 39 pp.

10. Bieniawski, Z. T., and W. L. van Heerden. The Significance of In Situ Tests on Large Rock Specimens. Int. J. of Rock Mech. Min. Sci. Geomech. Abstr., Apr. 1975, v. 12, No. 4, pp. 101-113.

11. Maleki, H. In Situ Pillar Strength and Failure Mechanisms for U.S. Coal Seams. Paper in Proceedings of the Workshop on Coal Pillar Mechanics and Design. USBM IC 9315, 1992, pp. 73-77.

12. Cox, R. M., T. L. Vandergrift, and J. P. McDonnell. Field Test of an Alternative Longwall Gate Road Design. USBM RI, 1994, in press.

13. Heasley, K. A., and J. C. Zelanko. Pillar Design in Bump-Prone Ground Using Numerical Models With Energy Calculations. Paper in Proceedings of the Workshop on Coal Pillar Mechanics and Design. USBM IC 9315, 1992, pp. 50-60.

14. Bieniawski, Z. T., and U. V. Vogler. Load-Deformation Behavior of Coal After Failure. Paper in Proceedings of the 2nd Int. Congr. on Rock Mechanics, ISRM, Belgrade, Yugoslavia, v. 1, 1970, paper #2-12.

15. Wagner, H. Determination of the Complete Load-Deformation Characteristics of Coal Pillars. Paper in Proceedings of the 3rd Int. Congr. on Rock Mechanics, Nat. Acad. Sci., v. 2B, 1974, pp. 1076-1081.

16. Van Heerden, W. L. In Situ Determination of Complete Stress-Strain Characteristics of Large Coal Specimens. J. S. Afr. Inst. Min. and Metall., v. 75, No. 8, 1975, pp. 207-217.

17. Skelly, W. A., J. Wolgamott, and F. D. Wang. Coal Pillar Strength and Deformation Prediction Through Laboratory Sample Testing. Paper in Proceedings of the 18th U.S. Symp. on Rock Mechanics, CO Sch. Mines, Golden, CO, 1977, pp. 2B5-1 to 2B5-5.

18. Das, M. N. Influence of Width/Height Ratio on Post Failure Behavior of Coal. Int. J. Min. and Geol. Engr., v. 4, 1986, pp. 79-87.

Special Publication 01-94

New Technology for Longwall Ground Control

Proceedings: U.S. Bureau of Mines Technology Transfer Seminar

Compiled by Christopher Mark, Robert J. Tuchman, Richard C. Repsher, and Catherine L. Simon

UNITED STATES DEPARTMENT OF THE INTERIOR
Bruce Babbitt, Secretary

BUREAU OF MINES

Cover Photograph: The U.S. Bureau of Mines has developed highly practical technologies for maintaining effective ground control in the hazardous tailgate entries of longwall mining systems, which will significantly improve the safety of the Nation's underground mineworkers. *(Photo: Alan A. Campoli, Pittsburgh Research Center, U.S. Bureau of Mines)*

For sale by the Superintendent of Documents, U.S. Government Printing Office
Washington, D.C. 20707